

- [17] M. Sasaki, T. Inoue, Y. Shirai, and F. Ueno, "Fuzzy multiple-input maximum and minimum circuits in current mode and their analyzes using bounded-difference equations," *IEEE Trans. Comput.*, vol. 39, pp. 768–778, June 1990.
- [18] T. Inoue, F. Ueno, T. Motomura, O. Setoguchi, and R. Matsuo, "New high-speed analogue max and min circuits using OTA-based bounded-difference operations," *Electron. Lett.*, vol. 27, pp. 1034–1035, June 1991.
- [19] G. Giustolisi, G. Palmisano, and G. Palumbo, "Analog fuzzy controller in SC technique," in *Proc. CSCC'99*, Athens, Greece, July 1999, pp. 363–368.
- [20] G. Giustolisi, G. Palmisano, and G. Palumbo, "Switched capacitor compatible minimum-maximum function," *Electron. Lett.*, vol. 36, pp. 35–36, Jan. 2000.

A High-Swing MOS Cascode Bias Circuit

Volney Coelho Vincence, Carlos Galup-Montoro, and
Márcio Cherm Schneider

Abstract—In this paper, we propose a very simple bias circuit that allows for maximum output voltage swing of MOSFET cascode stages. The circuit topology is valid for any current density and is technology independent. Starting from the saturation voltage as defined in [1], and from the current density of the cascode stage, we determine the aspect ratio of the transistors in the bias circuit in order to maximize the output voltage swing. Experimental results validate the strategy for designing the bias network.

Index Terms—Analog circuits, analog integrated circuits, biasing circuit, cascode amplifier, MOS analog integrated circuits.

I. INTRODUCTION

Cascode current mirrors (CCM) have a much higher output resistance than simple current mirrors yet at the expense of the output voltage swing. Self-biased CCM's [2], [3] have as their main drawback a very serious loss of signal swing. Cascode stages with fixed bias [4]–[7], such as those shown in Fig. 1 [8], [9], can be optimized for high output voltage swing. In order to maximize the output voltage swing, the values of the bias voltages V_{b1} , V_{b2} and V_{ref} should be such that M_4 , M_{10} , and M_i , respectively, operate at the edge of saturation.

Very simple circuits in [7] were proposed to bias cascode mirrors either for strong inversion or for weak inversion. The cascode biasing circuit proposed in [4] can operate at any current level with a minimal output saturation voltage but spends a lot of silicon area and is not suitable for high frequency applications.

In this brief, we extend for moderate and strong inversion one of the biasing circuits presented in [7], which was proposed for operation in weak inversion. The bias circuit proposed here is useful for both amplifier configurations shown in Fig. 1. In the first part of the brief, we revisit the MOSFET model from [1] and [10] and introduce a definition

Manuscript received January 2000; revised April 2000. This work was supported in part by CAPES and by CNPq. This paper was recommended by Associate Editor W. Serdijn.

V. C. Vincence is with the Department of Electrical Engineering, State University of Santa Catarina, CEP 89203-100, Joinville, SC, Brazil.

C. Galup-Montoro and M. C. Schneider are with the Department of Electrical Engineering, Federal University of Santa Catarina, CEP 88040-900, Florianópolis, SC, Brazil.

Publisher Item Identifier S 1057-7130(00)09933-X.

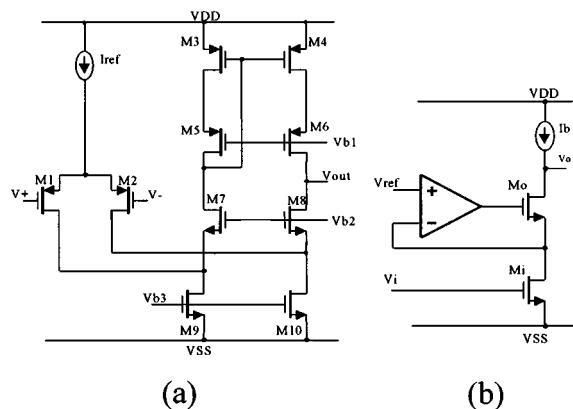


Fig. 1. (a) Folded cascode input stage [9]. (b) Cascoded gain stage with gain enhancement [8].

of the saturation voltage based on practical aspects of circuit design. Additionally, the small-signal output resistance is discussed and associated with the saturation voltage of the driver transistor in the CCM. The analysis of the biasing topology is discussed next. Design equations, as well as experimental results, are eventually presented.

II. THE SATURATION VOLTAGE

According to the MOSFET models in [1], [7], and [10], the drain current can be decomposed into the forward (I_F) and reverse (I_R) currents

$$I_D = I_F - I_R \quad (1)$$

where I_F (I_R) is dependent of the gate and source (drain) voltages. In forward saturation $I_F \gg I_R$; consequently, $I_D \cong I_F$.

The MOSFET output characteristic [1], [10] is modeled, in normalized form, as

$$\frac{V_{DS}}{\phi_t} = \sqrt{1 + i_f} - \sqrt{1 + i_r} + \ln \left(\frac{\sqrt{1 + i_f} - 1}{\sqrt{1 + i_r} - 1} \right) \quad (2)$$

where

$$i_{f(r)} = \frac{I_{F(R)}}{I_S} \quad (3a)$$

$$I_S = I_{SQ} \left(\frac{W}{L} \right) \quad (3b)$$

$$I_{SQ} = \mu n C'_{ox} \frac{\phi_t^2}{2}. \quad (3c)$$

I_S is the normalization current, I_{SQ} is the sheet normalization current, $i_{f(r)}$ is the normalized forward (reverse) current, and V_{DS} is the drain-to-source voltage. μ , n , C'_{ox} , ϕ_t , and W/L are the mobility, slope factor, gate oxide capacitance/area, thermal voltage, and the transistor aspect ratio, respectively. More details about (1)–(3) can be found in [1] and [10].

In order to introduce a definition of the saturation voltage that is useful for circuit designers, we first define $A = g_{ms}/g_{md}$, the voltage gain of the common-gate amplifier [Fig. 2(a)]. Here, g_{ms} is the source transconductance while g_{md} is the MOSFET output conductance. Indeed, "A" is equal to the ratio of the slope of the transistor output characteristic at the origin ($V_D = V_S$) to the slope of the characteristic at the operating point, as shown in Fig. 2. We now define the saturation voltage as the value of V_{DS} , for which the voltage gain of the common-gate amplifier equals A . Clearly, the so-called saturation

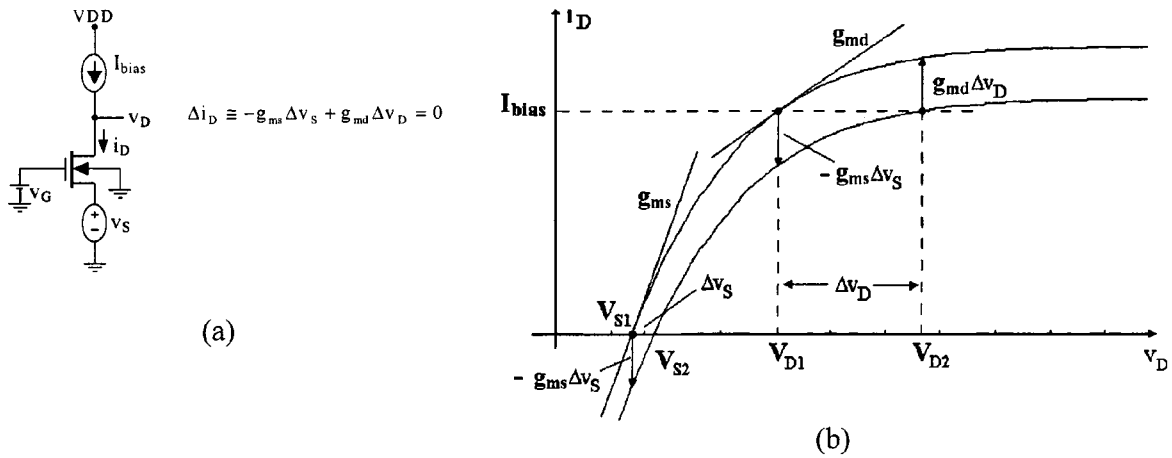


Fig. 2. (a) Common-gate amplifier. (b) Definition of the MOSFET source transconductance (g_{ms}) and output conductance (g_{md}).

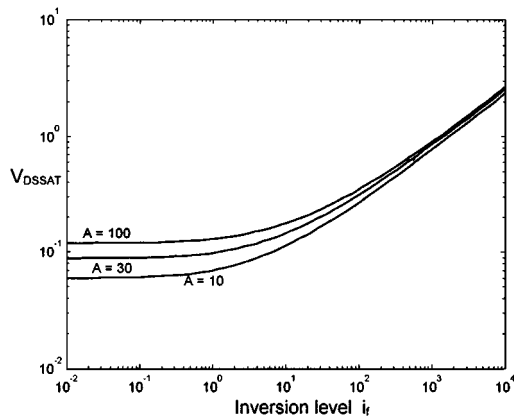


Fig. 3. Saturation voltage as a function of the inversion level, gain A as parameter, and $\phi_t = 26$ mV.

For large values of “ A ,” $i_f \gg i_r$, and, consequently, the normalized drain current $i_d = i_f - i_r \cong i_f$. Therefore, one can substitute i_d for i_f in (4b).

The definition of the saturation voltage as shown in (4b) is very appropriate for building blocks such as current mirrors where voltage swing and voltage gain are essential specifications. Fig. 3 illustrates the dependence of the saturation voltage on the inversion level. For strong-inversion $V_{DSSAT} \cong \phi_t \sqrt{i_f}$, while for weak-inversion $V_{DSSAT} \cong \phi_t \cdot \ln(A)$.

III. THE OUTPUT RESISTANCE

Cascode stages are capable of exhibiting very high output resistance and a gain-bandwidth product almost equal to that of a single stage [8]. With the aid of Fig. 4(a), one can readily determine the output impedance at the drain of $M4$

$$\frac{v_{out}}{i_{out}} \cong \frac{g_{ms4}/g_{md4}}{g_{md2}} \tag{5a}$$

The result in (5a) can be readily interpreted by noting that the ac drain voltage of $M2$ is equal to the ac output voltage divided by the voltage gain of the common-gate configuration. Assuming both $M2$ and $M4$ to be operating in saturation and to have the same aspect ratios, then $g_{ms4} \cong g_{ms2}$ [see (4a)]. Therefore, (5a) can be written as

$$\frac{v_{out}}{i_{out}} \cong \frac{g_{ms2}/g_{md2}}{g_{md4}} = \frac{A}{g_{md4}} \tag{5b}$$

where “ A ,” the voltage gain of $M2$ depends on the drain-source voltage, and thus, on the bias voltage V_B . Therefore, V_B should be sufficiently high to allow for a high “ A ” but not too high to avoid a reduction in the output voltage swing. The following section shows how to design the circuit in Fig. 4(b) to bias $M2$ at the edge of saturation.

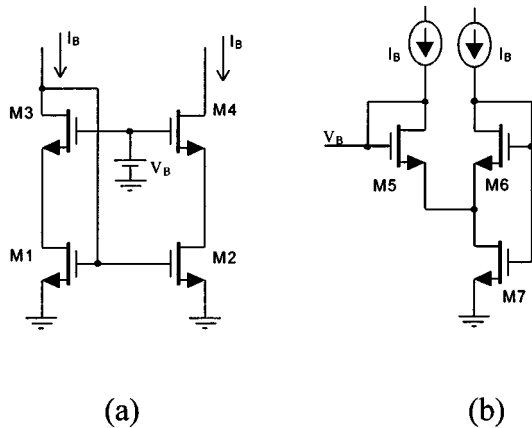


Fig. 4. (a) Low-voltage CCM. (b) Biasing circuit [7].

voltage should be associated with a large value of “ A .” Considering that

$$g_{ms(d)}\phi_t = 2I_S (\sqrt{1 + i_{f(r)}} - 1) \tag{4a}$$

as in [10], one can easily derive from (2) the value of the saturation voltage V_{DSSAT} [1] as

$$\frac{V_{DSSAT}}{\phi_t} = \ln(A) + \left(1 - \frac{1}{A}\right) (\sqrt{1 + i_f} - 1). \tag{4b}$$

IV. BIAS NETWORK

In the topology of the CCM shown in Fig. 4(a), all transistors share a common substrate. If V_B is adequately chosen, the output voltage of this circuit can be as low as $2V_{DSSAT}$. Biasing the transistors deep in weak inversion allows for low voltage operation and low power consumption but the frequency response is very poor. A balance between frequency response and voltage swing is achieved in moderate inversion.

The structure shown in Fig. 4(b), which has been proposed [7] to generate a bias voltage to allow for maximum output swing, is quite

choice of “ α ,” which defines the aspect ratio “ r ,” depends on the inversion level but is independent of the technological parameters. Note also that “ r ” ranges from 0.1–0.8 approximately. In strong inversion, the optimum value of r is 0.8 ($\sqrt{\alpha} = 1.5$). On the other hand, in weak inversion “ r ” varies from 0.1 to 0.5, depending on the value chosen for the voltage gain.

The bias network shown in Fig. 5 can be readily applied to the amplifiers shown in Fig. 1. For instance, the bias voltage V_{b2} in Fig. 1(a) is generated at the gate voltage of $MA5$. Additionally, the intermediate node of the series association of $MA5$ and $MB5$ provides the network of Fig. 1(b) with the appropriate voltage (V_{ref}) for maximum output swing.

Even though the present analysis has been performed for long-channel devices, we can apply it to short-channel devices as long as A is not higher than the maximum achievable gain of the short-channel device. Our analysis has not taken into account transistor or current mismatching. In a practical circuit, the aspect ratio r could be slightly decreased in order to add a small safety margin to the drain-source voltage of $M2$ that would compensate for transistor mismatching. The price to be paid would be a slightly smaller output voltage swing of the CCM.

V. EXPERIMENTAL RESULTS

To validate the design methodology, simple, self-biasing cascode (self-CCM) and low-voltage cascode (LV-CCM) current mirrors have been implemented and tested. Integrated N -channel transistors ($V_T \approx 0.6$ V) from a 2- μm CMOS technology have been used in the current mirrors. The measured sheet normalization current $I_{SQ} \approx 55$ nA. All transistors in the simple mirrors and CCM’s have the same aspect ratios ($W/L = 18 \mu\text{m}/5 \mu\text{m}$).

Figs. 7–9 present details of the measured output characteristics of the current mirrors. Values of $r = 1/3, 1/2,$ and $2/3$, respectively, have been chosen according to Fig. 6, for $i_f = 1, 10,$ and 100 and $A = 30$. Note that the LV-CCMs reach saturation at a drain-source voltage roughly twice the saturation voltage of the simple current mirror. The self-biased CCM saturates at a much larger voltage than the “optimally” biased CCM.

VI. CONCLUSION

In this work, the very simple bias circuit presented in [7], which allows for maximum output voltage swing of cascode stages in weak inversion, has been extended for operation at any current density. Starting from the multiplication factor of the output impedance required for the cascode stage relative to the single stage and from the output swing, one can determine the “optimally” biased network. The proposed biasing circuit, which is very useful for low-voltage design at any current level, is technology independent since it is based on geometric ratios. Experimental results corroborated the design methodology of the bias network.

REFERENCES

- [1] A. I. A. Cunha, M. C. Schneider, and C. Galup-Montoro, “An MOS transistor model for analog circuit design,” *IEEE J. Solid-State Circuits*, vol. 33, pp. 1510–1519, Oct. 1998.
- [2] E. Bruun and P. Shah, “Dynamic range of low-voltage cascode current mirrors,” in *Proc. ISCAS*, 1995, pp. 1328–1331.
- [3] F. You, S. H. K. Embabi, J. F. Duque-Carrillo, and E. Sánchez-Sinencio, “An improved tail current source for low voltage applications,” *IEEE J. Solid-State Circuits*, vol. 32, pp. 573–580, Aug. 1997.

- [4] P. Heim and M. A. Jabri, “MOS cascode-mirror biasing circuit operating at any current level with minimal output saturation voltage,” *Electron. Lett.*, vol. 31, pp. 690–691, Apr. 27, 1995.
- [5] T. Voo and C. Toumazou, “A novel high speed current mirror compensation technique and application,” in *Proc. ISCAS*, 1995, pp. 2108–2111.
- [6] T. C. Choi, R. T. Kaneshiro, R. W. Brodersen, P. R. Gray, W. B. Jett, and M. Wilcox, “High-frequency CMOS switched-capacitor filters for communications application,” *IEEE J. Solid-State Circuits*, vol. SSC-18, pp. 652–664, Dec. 1983.
- [7] E. Vittoz, “Micropower techniques,” in *Design of Analog-Digital VLSI Circuits for Telecommunications and Signal Processing*, 2nd ed, J. E. Franca and Y. Tsividis, Eds. Englewood Cliffs, NJ: Prentice-Hall, 1994.
- [8] K. Bult, “Basic CMOS circuit techniques,” in *Analog VLSI: Signal and Information Processing*, M. Ismail and T. Fiez, Eds. New York: McGraw-Hill, 1994.
- [9] R. Hogervorst and J. H. Huijsing, *Design of Low-Voltage, Low-Power Operational Amplifier Cells*. Norwell, MA: Kluwer, 1996.
- [10] C. Galup-Montoro, M. C. Schneider, and A. I. A. Cunha, “A current-based MOSFET model for integrated circuit design,” in *Low-Voltage/Low-Power Integrated Circuits and Systems*, E. Sánchez-Sinencio and A. G. Andreou, Eds. New York: IEEE Press, 1999.

Analog VLSI Implementation of the Help If Needed Stereopsis Algorithm

Albert H. Titus and Timothy J. Drabik

Abstract—This brief introduces a novel clocked analog VLSI hardware system with an optical input that performs stereopsis. An algorithm called the Help If Needed Algorithm, developed previously, is readily mapped onto an analog VLSI platform. The system fits into the cellular neural network (CNN) paradigm. The circuit components that make up the cells of the CNN are designed with the constraint that they must function effectively and fit into the space available. In order to clarify the processing pathway, the system is described at the component and system levels. Each cell has an optical input, while the output is electrical. By utilizing an optical input, an analog VLSI silicon retina first stage can be connected to the stereopsis processor completely in parallel, creating a multi-stage artificial visual system. The physical system is composed of 2.0 μm Tinchips fabricated through MOSIS. Experimental data are presented that verify that the system performs as desired and successfully implements the Help If Needed Stereopsis Algorithm. The novel stereopsis processor is ideally suited for autonomous robots, or any application that requires a low power visual processing system.

Index Terms—Analog processing circuits, CMOS analog integrated circuits, machine vision, neural network hardware, very large scale integration.

I. INTRODUCTION

An important visual-processing task performed by biological systems is the determination of depth. Depth perception can be achieved using a number of methods, but one of the most efficient methods is stereopsis. Disparate information is present at each eye, and the slight differences in the images are used to determine how close or far an

Manuscript received July 1999; revised July 2000. This paper was recommended by Associate Editor A. Rodriguez-Vazquez.

The author is with the Department of Electrical Engineering, Rochester Institute of Technology, James E. Gleason Building, Rochester, NY 14623-5603 USA (e-mail: ahtee@rit.edu).

Publisher Item Identifier S 1057-7130(00)09931-6.